

Response to reviewers for the paper “Nitrate radical generation via continuous generation of dinitrogen pentoxide in a laminar flow reactor coupled to an oxidation flow reactor.”

We thank the referee for his/her comments on our paper. To guide the review process, we have copied the referee’s comments in black text. Our responses are in blue text. Alterations to the paper are indicated in bold text below and in annotations to the revised manuscript.

Anonymous Referee #1

General comments

1. Regarding the NO_3 estimation equation for the OFR- iN_2O_5 , I wonder how would multiple generation oxidations influence the estimation of NO_3 exposure. For example, NO_3 radical oxidation of typical BVOCs (isoprene, monoterpenes, sesquiterpenes) produces carbonyls and even products with carbon double bonds. These products are highly reactive toward NO_3 radicals which may affect the NO_3 exposure estimation. However, these are not considered in the KimSim simulations. Secondly, NO_3 oxidation of BVOCs has high SOA yields. I wonder how the uptake of NO_3 and N_2O_5 by the produced particles affect the simulations.

We added the following text to the end of Section 3.5:

P10, L24: “ $(\text{NO}_3\text{R})_{\text{ext}}$ of a system will change over the course of multiple generations of NO_3 oxidation due to changes in kinetic rate coefficients between different species and NO_3 (k_{NO_3}). The sensitivity of Eq. 5 to changes in $(\text{NO}_3\text{R})_{\text{ext}}$ depends in part on the relative magnitudes of $(\text{NO}_3\text{R})_{\text{ext}}$ and the internal NO_3 reactivity, $(\text{NO}_3\text{R})_{\text{int}}$, which is approximately equal to $k_{\text{NO}_2+\text{NO}_3}[\text{NO}_2]$. If $(\text{NO}_3\text{R})_{\text{int}} \gg (\text{NO}_3\text{R})_{\text{ext}}$, changes in $(\text{NO}_3\text{R})_{\text{ext}}$ would have minimal influence on Eq. 5.

In one case study, we examined changes in $(\text{NO}_3\text{R})_{\text{ext}}$ following conversion of biogenic VOCs (BVOCs) to gas-phase carbonyl oxidation products with known k_{NO_3} values. Table S5 compares k_{NO_3} of isoprene to methyl vinyl ketone and methacrolein, α -pinene to pinonaldehyde, sabinene to sabinaketone, and 3-carene to caronaldehyde. In the limit where 100% of each BVOC is converted to its carbonyl oxidation product(s), $(\text{NO}_3\text{R})_{\text{ext}}$ decreases by a factor of 200 or greater. Unsaturated organic nitrates that are generated from $\text{BVOC} + \text{NO}_3$ may also be reactive towards NO_3 , but k_{NO_3} for these species are not available.

In another case study, we examined changes in $(\text{NO}_3\text{R})_{\text{ext}}$ following conversion of BVOCs to SOA. An effective k_{NO_3} for SOA was calculated using the following equation adapted from Lambe et al. (2009):

$$k_{\text{NO}_3} = \frac{3}{2} \frac{\gamma \times \bar{c} \times M_{\text{SOA}} \times F_{\text{diff}}}{D_p \times \rho_p \times N_A}$$

where F_{diff} is a correction factor accounting for diffusion limitations to the particle surface in the transition regime (Fuchs and Sutugin, 1970):

$$F_{\text{diff}} = \frac{1 + 6 \times \frac{D_{\text{NO}_3}}{\bar{c} \times D_p}}{1 + 10.26 \times \frac{D_{\text{NO}_3}}{\bar{c} \times D_p} + 47.88 \times \left(\frac{D_{\text{NO}_3}}{\bar{c} \times D_p} \right)^2}$$

and γ is the fraction of collisions between NO_3 and SOA leading to reaction, D_p is the surface area-weighted mean particle diameter, ρ_p is the particle density, N_A is Avogadro’s number, c is the mean molecular speed of NO_3 ($3.2 \times 10^4 \text{ cm s}^{-1}$ at $T = 298 \text{ K}$), M is the mean molecular weight of the SOA, and $D_{\text{NO}_3} = 0.08 \text{ cm}^2 \text{ s}^{-1}$ is

the NO_3 diffusion coefficient in air (Rudich et al., 1996). Figure S4 shows $k_{\text{SOA}+\text{NO}_3}$ as a function of D_p ranging from 1 to 1000 nm assuming $\rho_p = 1.4 \text{ g cm}^{-3}$, $M_{\text{SOA}} = 250 \text{ g mol}^{-1}$ (Nah et al., 2016) and an upper limit $\gamma = 0.1$ for BVOC-derived SOA (Ng et al., 2017). For reference, the range of slowest (isoprene) and fastest (humulene) $k_{\text{BVOC}+\text{NO}_3}$ are indicated by the vertical blue line on the y-axis. In the limit where 100% of a BVOC is converted to SOA, $(\text{NO}_3\text{R})_{\text{ext}}$ decreases by a factor of 10 or greater depending on $k_{\text{BVOC}+\text{NO}_3}$ and D_p .

Taken together, these results suggest that $(\text{NO}_3\text{R})_{\text{ext}}$ decreases following NO_3 oxidation of BVOCs to carbonyl oxidation products and/or SOA. In this case, inputting $(\text{NO}_3\text{R})_{\text{ext}}$ of the BVOC precursor to Eq. 5 generates a lower limit to $(\text{NO}_3)_{\text{exp}}$ over multiple generations of NO_3 oxidation. Results for other systems will depend on k_{NO_3} values of associated gas- and condensed-phase precursors and their oxidation products.”

Table S5 and Figure S4 were added to the supplement:

Table S5. Bimolecular rate coefficients between selected biogenic volatile organic compounds (BVOCs) and NO_3 , and BVOC + NO_3 carbonyl oxidation products and NO_3 . Rate coefficients were obtained from Ng et al. (2017) and references therein, and are given in units of $\text{cm}^3 \text{ molecules}^{-1} \text{ s}^{-1}$.

BVOC	k_{NO_3}	Oxidation Product	k_{NO_3}
isoprene	6.5×10^{-13}	methyl vinyl ketone	$< 6 \times 10^{-16}$
		methacrolein	3.4×10^{-15}
α -pinene	6.2×10^{-12}	pinonaldehyde	2.0×10^{-14}
3-carene	9.1×10^{-12}	caronaldehyde	2.5×10^{-14}
sabinene	1.0×10^{-11}	sabinaketone	3.6×10^{-16}

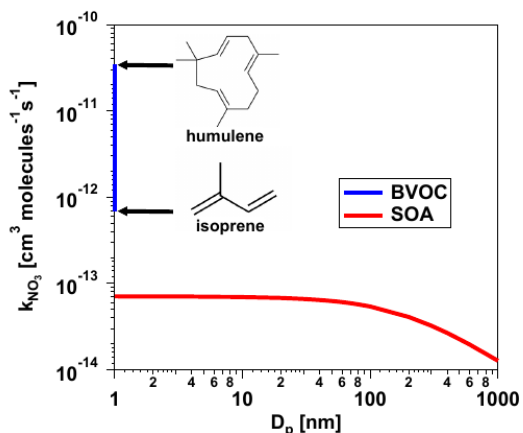


Figure S4. Effective rate constant between NO_3 and SOA particles (k_{NO_3}) calculated using Eq. 6 assuming $\rho_p = 1.4 \text{ g cm}^{-3}$, $M_{\text{SOA}} = 250 \text{ g mol}^{-1}$ and $\gamma = 0.1$.

The following citations were added to references:

N. A. Fuchs and A. G. Sutugin: Highly Dispersed Aerosols, Ann Arbor Science Publishers, Newton, MA, 1970.

A. T. Lambe, M. A. Miracolo, C. J. Hennigan, A. L. Robinson, and N. M. Donahue, Effective Rate Constants and Uptake Coefficients for the Reactions of Organic Molecular Markers (*n*-Alkanes, Hopanes, and

Steranes) in Motor Oil and Diesel Primary Organic Aerosols with Hydroxyl Radicals, *Environ. Sci. Technol.* 43(23) 8794-8800, <https://doi.org/10.1021/es901745h>, 2009.

Y. Rudich, R. K. Talukdar, T. Imamura, R.W. Fox, and A.R. Ravishankara, Uptake of NO₃ on KI solutions: rate coefficient for the NO₃ + I⁻ reaction and gas-phase diffusion coefficients for NO₃, *Chem. Phys. Lett.*, 261(4-5), 467-473, [https://doi.org/10.1016/0009-2614\(96\)00980-3](https://doi.org/10.1016/0009-2614(96)00980-3), 1996.

Specific comments:

- 2) BBCES measuring the NO₃:
 - a. The author stated that “ $I(\lambda)$ and $I_0(\lambda)$ were the measured transmitted intensities in the presence and absence of NO₃”. How was the “absence of NO₃” achieved?

This is now specified in the text (p4, L16) (see below).

- b. The equation grading the calculation of $\alpha(\lambda)$ is not correct. The $\alpha(\lambda)$ in the cavity also contributed by the bath gas beyond the NO₃ radicals.

The equation is correct. Additional of information is now provided in the text to avoid any misunderstanding in the equation.

We modified the text as follows (changes bolded):

P4, L4: direct measurements of NO₃ generated via OR-iN₂O₅ were performed using a newly developed Incoherent Broad Band Cavity Enhanced Absorption Spectroscopy (IBBCEAS) technique (Cirtog et al., manuscript in preparation, **Fouqueau et al., 2020**).

P4, L11: Briefly, measurements were conducted by exciting a high-finesse optical cavity formed by two high reflectivity mirrors with an incoherent broad-band-source centered on the $\lambda = 662$ nm absorption cross section of NO₃ (2×10^{-17} cm², **Orphal et al., 2003**).

P4, L16: “**Where $\alpha(\lambda)$ is the absorption coefficient of the OFR sample in the instrument, $I(\lambda)$ and $I_0(\lambda)$ were the measured transmitted intensities in the presence and absence of the sample, $d = 61$ was the distance between the cavity mirrors, and $R(\lambda)$ was the mirror reflectivity ($\sim 99.98\%$). $I_0(\lambda)$ was obtained by stopping the OFR sample through the instrument and flowing nitrogen from a cylinder (Air Liquide). A period of at least 30 s was allowed between the measurement of $I_0(\lambda)$ and $I(\lambda)$ to ensure the complete purge of the instrument. $R(\lambda)$ was measured before each experiment using a certified calibration cylinder containing 600 ppb NO₂ in zero air (Air Liquide).**”

- c. The NO₃ radicals are highly reactive and can easily lose to the walls. What is the transmission efficiency of NO₃ from the OFR to the cavity?
 - d. Due to different loss rates of NO₃ and N₂O₅ to the wall, the equilibrium of NO₃ and N₂O₅ may change. How good is the measured NO₃ concentration in the CRD represent the NO₃ radical concentration in the reactor?

We modified the text as follows (changes bolded):

P4, L20-27: “ Concentrations were calculated by applying a least square fit to the measured $\alpha(\lambda)$ considering the absorbing species in the sample:

$$\alpha(\lambda) = [NO_2]\sigma_{[NO_2]}(\lambda) + [NO_3]\sigma_{[NO_3]}(\lambda) + [O_3]\sigma_{[O_3]} + p(\lambda)$$

with NO_2 , NO_3 and O_3 being the species absorbing in the spectral region of the instrument, $\sigma(\lambda)$ are the respective absorption cross sections convoluted with the apparatus function (Vandaele et al., 1998; Orphal et al., 2003, Voigt et al, 2001) and $p(\lambda)$ is a cubic polynomial to correct baseline deformations due to small LED intensity variations. To avoid saturation of the IBBCEAS in these experiments, the OFR sample was diluted by a controlled dilution factor ranging from 9 to 41 and the detection response was deliberately lowered by reducing the optical path length. Sampling lines and instrument (cavity) were made of PFA. The residence time in the IBBCEAS sampling line and instrument ranged from 8.3 to 21.8 s. At these residence times, the calculated transmission efficiency of NO_3 from the OFR to the IBBCEAS instrument ranged from 0.3 to 11% assuming a NO_3 wall loss rate constant of 0.27 s^{-1} (Kennedy et al., 2011). Corrections to measured NO_2 and NO_3 values accounting for N_2O_5 thermal decomposition, N_2O_5 wall loss, and sample dilution in the IBBCEAS inlet were additionally applied to results presented in this paper.”

The following citations were added to references:

Fouqueau, A., Cirtog, M., Cazaunau, M., Pangui, E., Zapf, P., Siour, G., Landsheere, X., Méjean, G., Romanini, D. and Picquet-Varrault, B.: Implementation of an IBBCEAS technique in an atmospheric simulation chamber for in situ NO_3 monitoring: characterization and validation for kinetic studies, Atmos Meas Tech, (amt-2020-103), in review, 2020.

S. Voigt, J. Orphal, K. Bogumil, and J.P. Burrows, "The temperature dependence (203-293 K) of the absorption cross sections of O_3 in the 230-850 nm region measured by Fourier-transform spectroscopy", J. Photochem. Photobiol. A: Chem. 143, 1-9 (2001); DOI: [10.1016/S1010-6030\(01\)00480-4](https://doi.org/10.1016/S1010-6030(01)00480-4)

- 3) a) The description of the results in section 3.4 is not consistent with the results in the figure. “First, at $[O_3]_{0,LFR} < 1000 \text{ ppm}$ and $[NO_2]_{0,LFR}:[O_3]_{0,LFR} = 0.1$ to 1.8, maximum NO_{3exp} increased with decreasing $[NO_2]_{0,LFR}:[O_3]_{0,LFR}$ (Fig. 7a).” It is very hard to see the results in the figure when $[O_3]_{0,LFR} < 100 \text{ ppm}$. For me, it looks like maximum NO_{3exp} first increase with increasing $[NO_2]_{0,LFR}:[O_3]_{0,LFR}$ ratio and then decrease with it, especially when $[O_3]_{0,LFR}$ was in the range of 100-1000ppm”

We modified the text as follows:

“First, at $[O_3]_{0,LFR} < 1000 \text{ ppm}$ and $[NO_2]_{0,LFR}:[O_3]_{0,LFR} = 0.01$ to 1.8, maximum NO_{3exp} increased with $[NO_2]_{0,LFR}:[O_3]_{0,LFR}$ prior to decreasing at $[NO_2]_{0,LFR}:[O_3]_{0,LFR} > 1.0$ (Fig. 7a).”

b) “Above $[O_3]_{0,LFR} \approx 2000 \text{ ppm}$, NO_{3exp} was less sensitive to $[NO_2]_{0,LFR}:[O_3]_{0,LFR}$.” This is true except for $[NO_2]_{0,LFR}:[O_3]_{0,LFR} = 2.0$.

We modified the text as follows:

“Above $[O_3]_{0,LFR} \approx 2000 \text{ ppm}$ and below $[NO_2]_{0,LFR}:[O_3]_{0,LFR} = 2.0$, NO_{3exp} was less sensitive to $[NO_2]_{0,LFR}:[O_3]_{0,LFR}$.”

c) “Second, maximum NO₃:O₃ increased with increasing [NO₂]_{0,LFR}: [O₃]_{0,LFR} (Figure 7c).” This statement is true only when the O₃ was above 1000 ppm, even get rid of the results from [NO₂]_{0,LFR}: [O₃]_{0,LFR}=2.0.

We modified the text as follows:

“Second, maximum NO₃:O₃ increased with increasing [NO₂]_{0,LFR}: [O₃]_{0,LFR} **above [O₃]_{0,LFR} = 1000 ppm** (Figure 7c).”

d) “conversion of O₃ to N₂O₅ inside the LFR” I fell more comfortable to say “conversion of O₃ to O₂ inside the LFR”.

We modified the text as follows:

“conversion of O₃ to O₂ inside the LFR”

- 4) The authors tried to investigate the RO₂ fate and considered “RO₂ react with NO, NO₂, NO₃, HO₂, or other RO₂ to generate alkoxy (RO) radicals, peroxy nitrates (RO₂NO₂), hydroperoxides or organic peroxides, and may additionally undergo autooxidation via sequential isomerization and O₂ addition.” Recent studies by Berndt et al. (2018) revealed that self-and cross-reaction of RO₂ radicals would produce dimers effectively. How could this process affect the fate of the RO₂ radical?

Self- and cross-reactions of RO₂ were considered in the model – please see the last two rows in Table S3, reproduced below for reference. Under the conditions that were studied this process was minor compared to RO₂ + NO₃ and RO₂ + NO₂.

Table S3. KinSim mechanism used to model destruction of alkyl and acyl organic peroxy radicals formed from VOC + NO₃ reactions in the OFR. Kinetic data is adapted from (Orlando and Tyndall, 2012).

Reactant 1	Reactant 2	Product 1	Product 2	Product 3	A _∞	E _∞	n _∞	A ₀	E ₀	n ₀
VOC	NO ₃	alkylRO2			0 or 2.5E-12	0	0	0	0	0
VOC	NO ₃	acylRO2			2.5E-12 or 0	0	0	0	0	0
alkylRO2	NO				2.7E-12	-360	0	0	0	0
acylRO2	NO				7.5E-12	-290	0	0	0	0
alkylRO2	NO ₂	alkylRO2NO ₂			6.1E-12	0	0	1.3E-30	6.2	0.31
alkylRO2NO ₂		alkylRO2	NO ₂		8.8E+15	10440	0	0.00048	9285	0.31
acylRO2	NO ₂	acylRO2NO ₂			1.2E-11	0	0.9	2.7E-28	7.1	0.3
acylRO2NO ₂		acylRO2	NO ₂		5.4E+16	13830	0	0.0049	12100	0.3
alkylRO2	NO ₃	alkylRO	NO ₂		2.4E-12	0	0	0	0	0
acylRO2	NO ₃	acylRO	NO ₂		3.2E-12	0	0	0	0	0
alkylRO2	HO ₂				7.4E-13	-700	0	0	0	0
acylRO2	HO ₂				5.2E-13	-980	0	0	0	0
alkylRO2	acylRO2				2.2E-12	-500	0	0	0	0
acylRO2	acylRO2				2.9E-12	-500	0	0	0	0

In response to the reviewer’s comment, we conducted additional sensitivity studies where the RO₂ + RO₂ rate constant was assumed to be 1x10⁻¹⁰ cm³ molecule⁻¹ s⁻¹, close to the values reported by Berndt et al. (2018). The sensitivity cases cover the range of conditions used in Section 3.4 and those with NO₃R_{ext} (and

hence VOC concentration) increased by a factor of 10. In these cases, the relative contribution of RO₂ + RO₂ to RO₂ fate is always <1%. To include this information in the paper, we modified the text as follows:

P8, L23-25: “Under almost all OFR-iN₂O₅ conditions shown in Figure 7, RO₂ reactions with NO, HO₂, and RO₂ were minor (< 1%) loss pathways compared to reaction with NO₂ and NO₃. **We conductive a model sensitivity analysis in which the RO₂ + RO₂ reaction rate was enhanced by increasing NO₃R_{ext} from 0.07 to 0.7 s⁻¹ and increasing the RO₂ + RO₂ rate constant from 1x10⁻¹¹ to 1x10⁻¹⁰ cm³ molecule⁻¹ s⁻¹ (Berndt et al., 2018, 2018a). Despite these perturbations, the relative contribution of RO₂ + RO₂ reactions to total RO₂ loss remained < 1% across this range of OFR-iN₂O₅ conditions.”**

The following citations were added to References:

Berndt, T.; Mentler, B.; Scholz, W.; Fischer, L.; Herrmann, H.; Kulmala, M.; Hansel, A., Accretion Product Formation from Ozonolysis and OH Radical Reaction of alpha-Pinene: Mechanistic Insight and the Influence of Isoprene and Ethylene. Environ. Sci. Technol. 2018, 52, (19), 11069-11077.

Berndt, T.; Scholz, W.; Mentler, B.; Fischer, L.; Herrmann, H.; Kulmala, M.; Hansel, A., Accretion Product Formation from Self- and Cross-Reactions of RO₂ Radicals in the Atmosphere. Angew Chem Int Edit 2018, 57, 1, 3820-3824.